NANO LETTERS

pubs.acs.org/NanoLett

Letter

The Fine-Structure Constant as a Ruler for the Band-Edge Light Absorption Strength of Bulk and Quantum-Confined Semiconductors

P. Tim Prins,[#] Maryam Alimoradi Jazi,[#] Niall A. Killilea, Wiel H. Evers, Pieter Geiregat, Wolfgang Heiss, Arjan J. Houtepen, Christophe Delerue, Zeger Hens, and Daniel Vanmaekelbergh*

Cite This: *Nano Lett.* 2021, 21, 9426−9432

Read Online

ACCESS | Metrics & More | Article Recommendations | Supporting Information

ABSTRACT: Low-dimensional semiconductors have found numerous applications in optoelectronics. However, a quantitative comparison of the absorption strength of low-dimensional versus bulk semiconductors has remained elusive. Here, we report generality in the band-edge light absorptance of semiconductors, independent of their dimensions. First, we provide atomistic tight-binding calculations that show that the absorptance of semiconductor quantum wells equals $m\pi\alpha$ (m = 1 or 2 with α as the fine-structure constant), in agreement with reported experimental results. Then, we show experimentally that a monolayer (superlattice) of quantum dots has similar absorptance, suggesting an absorptance quantum of $m\pi\alpha$ per (confined) exciton diameter. Extending this idea to bulk semiconductors, we experimentally demonstrate that an absorptance quantum equal to $m\pi\alpha$ per exciton Bohr diameter explains their widely varying absorption coefficients. We thus provided compelling evidence that the absorptance quantum $\pi\alpha$ per exciton diameter rules the band-edge absorption of all direct semiconductors, regardless of their dimension.

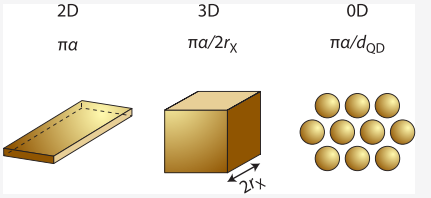

KEYWORDS: *fine-structure constant, optical transitions, light absorption, dielectric screening, quantum coupling*

Low-dimensional semiconductors and quantum wells play a key role in optoelectronic devices, such as infrared photodetectors, solar cells, lasers, and phosphors in displays and LEDs.[1−7] Optical transitions over the fundamental gap involve the valence hole and conduction electron states. The absorption and emission spectra depend on the semiconductor band structure and thus on the degree of electron (hole) confinement. Regarding the energetics of optical transitions, the effects of quantum confinement have been extensively studied, and this knowledge has resulted in a tremendous series of applications. The effects of confinement on the rate or strength of optical transitions are less documented and especially for band-edge absorption, a quantitative comparison between semiconductor nanostructures and bulk semiconductors is still very much needed. For one thing, such an analysis is hampered by the impact of dielectric screening on transition rates. For instance, for zero-dimensional (0D) quantum dots (QDs), the dielectric contrast between the semiconductor and its surroundings leads to a substantial reduction of the incident electromagnetic field within the QD, which lowers the effective transition rates.[8−11] Considering quasi-spherical QDs, a systematic correction for screening effects made clear that QDs exhibit similar absorption coefficients as the corresponding bulk semiconductors at energies where quantum confinement is negligible.[10] But a quantitative comparison on the strength of band-edge absorption and the effects of quantum confinement on this is lacking, although semiconductor QDs are often qualified as "strong" absorbers and emitters. The band-edge transition in QDs is typically characterized by an oscillator strength or integrated cross section, not unlike a two-level system (see Supporting Information S1). These quantities are valid as descriptors. However, these quantities obscure possible similarities or differences with band-edge absorption in bulk semiconductors, which is typically described by an absorption coefficient.

Here, we use the notion of absorptance per active element, that is, the volume of the electron−hole exciton, to compare the band-edge absorption strength of a wide variety of direct semiconductors from three-dimensional (3D) bulk semiconductors to 0D QDs. This means that for 0D QDs we measure the absorptance of a compact monolayer of QDs to obtain the absorptance per confined exciton volume; for bulk semiconductors, we derive the absorptance per bulk exciton volume from the absorption coefficient spectrum and the exciton Bohr diameter, obtained from the effective electron and hole mass. As a starting point, we reconsider the absorptance of two-dimensional (2D) semiconductors (quantum wells) in which the exciton experiences confinement in the

Received: July 10, 2021
Revised: November 9, 2021
Published: November 15, 2021

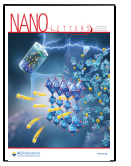

https://doi.org/10.1021/acs.nanolett.1c02682
Nano Lett. 2021, 21, 9426−9432

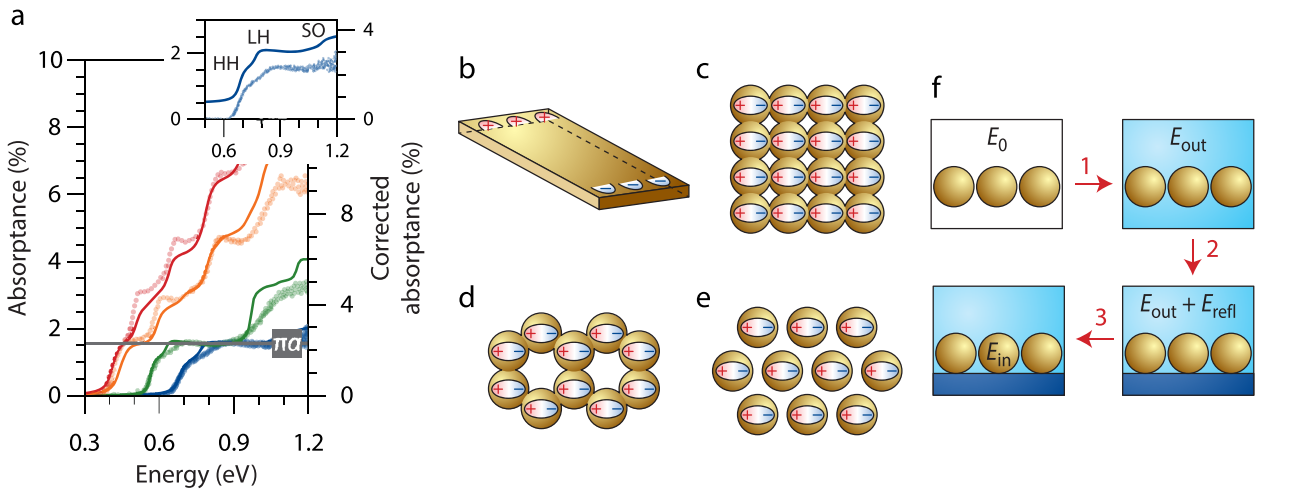

Figure 1. Measured and calculated absorptance of InAs quantum wells, and a schematic representation of the screening of the electromagnetic field in a quantum well and a QD monolayer. (a) Measured absorptance spectra of InAs quantum wells with variable thickness; 6 nm (blue), 9 nm (green), 14 nm (orange), and 19 nm (red) (data from ref 12). The thick solid lines represent the absorptance spectra calculated with an atomistic tight-binding model in which we have slightly adjusted the quantum well thickness to match the optical threshold with the measured one (details and justification in SI). The right axis provides the absorptance corrected for substrate reflection (see text and below). For all experimental and calculated spectra, the absorptance of the first allowed transition (and subsequent steps) is equal to $\pi\alpha$. The inset shows the experimental and calculated absorption spectra for a 6 nm thick InAs quantum well in more detail. The calculated spectrum is shifted with 0.5% for clarity. The labels are the transitions from the heavy-hole (HH), light-hole (LH), and spin−orbit split-off band (SO) to the lowest conduction band. (b−e) Comparison of the reduction of the electromagnetic field by dynamic charge accumulation (dielectric screening) in a quantum well (no screening | $F|^2 = 1$), a square superlattice $|F|^2 = 0.59$, and a honeycomb quantum dot superlattice, $|F|^2 = 0.36$. (f) A schematic overview of the photonic effects that results in a screening of the electromagnetic field. Step 1 induces a factor $1/n_m$ on the absorptance, n_m the refractive index of the surrounding medium. Step 2 includes the effect of reflection in case a substrate with refractive index n_s is present, resulting in a factor $4n_m^2/(n_s + n_m)^2$. The third step is the screening of the dielectric field inside the QDs, reducing the squared field strength with a factor $|F|^2$.

direction perpendicular to the well. The absorptance of InAs quantum wells of different thicknesses has been reported to increase in steps of $\pi\alpha$, with $\alpha = e^2/4\pi\varepsilon_0\hbar c$ being the fine-structure constant.[12] We show by means of atomistic tight-binding calculations that this "quantum of absorption" characterizes the absorptance of a multitude of 2D semiconductors, which invariably exhibits steps with increasing photon energy of $m\pi\alpha$ with $m = 1$ or 2, depending on the nature of the conduction- and valence-band valleys. By generalizing literature results,[11−14] this outcome urged us to investigate the absorptance of 0D QDs; we therefore designed QD samples in which the absolute band-edge absorptance can be measured in the same way as for the 2D quantum wells. After correction for photonic effects, we report that the absorptance per QD is close to $m\pi\alpha$. Finally, we develop a heuristic model to frame these remarkable results. For bulk semiconductors, the model suggests an absorptance of $m\pi\alpha$ per Bohr exciton diameter. We confirm this by using reported values of the band edge absorption coefficients for many different semiconductors spread over 2 orders of magnitude. We thus show empirically that the absorptance quantum $\pi\alpha$ is a good ruler to estimate the band-edge absorption strength of all direct semiconductors, independent of the degree of quantum confinement, if we consider the exciton volume as the elementary optically active volume.

TWO-DIMENSIONAL SEMICONDUCTORS

With InAs quantum wells as an example, it was experimentally shown that the absorptance increases stepwise with the photon energy with steps equal to $\pi\alpha$,[12] see Figure 1a. The InAs quantum wells of different thickness were grown on a CaF_2 substrate, each showing pronounced steps equal to 1.6% in the absorptance spectrum. To address intrinsic material properties, however, this result has to be corrected for reflection from the substrate by a factor $4n_m^2/(n_s + n_m)^2$, where n_m is the refractive index of the medium (air, $n_m = 1$) and n_s is the refractive index of the substrate (CaF_2, $n_s = 1.43$), see Figure 1. Each step in the absorptance amounts then to $\pi\alpha$, that is, $\pi/137 = 2.3\%$. Importantly, in this quasi-2D configuration, the semiconductor itself does not screen the electromagnetic field for light perpendicularly incident on the quantum well surface.

In ref 12, it was argued that this remarkably simple result follows from applying Fermi's golden rule within a $k\cdot p$ description of a set of nondegenerate energy bands for which many factors in the transition dipole matrix element and the joint density of states mutually cancel, see also Supporting Information S2. However, we found that this result has a more general meaning and is not due to coincidental simplifications in the effective mass theory. We performed atomistic tight-binding calculations for an InAs quantum well (of varying thickness) in the single-particle regime (see Supporting Information S2). As shown in Figure 1a, the tight-binding calculated absorptance spectra (thick solid lines) show overall steps of close to $\pi\alpha$. However, a close watch shows some fine structure in the first plateau, and due to the transitions of the heavy-hole, light-hole, and spin−orbit split-off band to the lowest conduction band, all three transitions contribute to an overall absorptance of close to $\pi\alpha$. With the understanding of these features in the atomistic tight-binding calculations, we now also recognize these features in the experimental data from ref 12. The inset in Figure 1a shows the experimental and calculated absorptance spectra of a 6 nm thick InAs quantum well in more detail. Atomistic tight-binding calculations account for deviations of parabolicity of the bands for the existence of heavy- and light-hole bands with anisotropic warping and for the mixing of these band states due to the

https://doi.org/10.1021/acs.nanolett.1c02682
Nano Lett. 2021, 21, 9426−9432

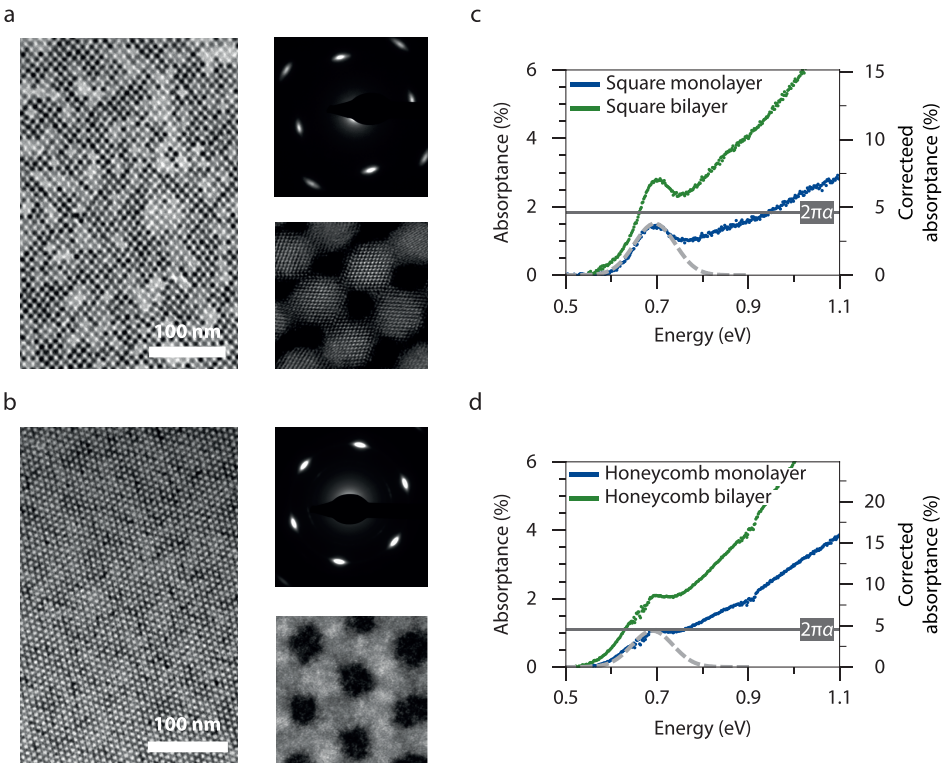

Figure 2. Absorptance of quantum dot monolayer superlattices. (a) TEM image of a part of a PbSe square superlattice taken from the sample also used in the absorptance measurements. Lower right insert: HAADF-STEM images of the superlattice showing the epitaxial connection of the QDs. Top right insert: Electron diffraction pattern showing atomic alignment between the QDs. (b) TEM image of a part of a PbSe superlattice with silicene-type honeycomb geometry. Lower right inset: HAADF-STEM image showing the epitaxial connection between the QDs and the hexagonal array of voids in the superlattice. Top left inset: Electron diffraction pattern showing atomic alignment between the QDs, oriented with the [111] axis upward. (c) Absorptance (%) as a function of photon energy for a square PbSe superlattice (blue, one monolayer in thickness) present on a quartz substrate, the absorptance is 1.5% at 0.7 eV. The green spectrum shows the absorptance when a second PbSe square superlattice is stacked on the first one. (d) Absorptance for one layer of the honeycomb superlattice (blue); the absorptance is 1.1% at a photon energy of 0.7 eV. The addition of one more honeycomb monolayer (green) adds a similar contribution to the absorptance as the first monolayer. In both panels c and d, the right *y*-axis shows the bare absorptance, thus corrected for photonic effects. In both cases, the bare absorptance at 0.7 eV is close to $2\pi\alpha$. This is very similar to the result calculated with an atomistic tight-binding model for PbSe quantum wells. The light gray dashed lines in panels c and d show the absorptance feature calculated from the known integrated absorption cross section (Supporting Information S1).

quantum confinement. In order to find out if this result is independent of the semiconductor material, we have calculated the absorptance for specific II−VI and IV−VI compounds as well. As shown in Supporting Information S2, CdSe quantum wells also feature absorptance steps of $\pi\alpha$, while the absorptance of PbSe quantum wells is characterized by steps of $2\pi\alpha$. We assign the latter finding to a combination of a 4-fold degenerate bandgap at the L points of the Brillouin zone and the quasi-linear dispersion relation of the valence and conduction bands around the L points. We thus find in general that the absorptance of direct 2D semiconductors equals $\mathcal{A}_{2D} = m\pi\alpha$ with $m = 1$ or $m = 2$, depending on the nature of the band edges.

MONOLAYER QD SUPERLATTICES

In the very active field of colloidal QDs, the size-dependence and inhomogeneous broadening of the band-edge absorptance as measured on QD suspensions has been extensively investigated. However, the absorption of light resonant with the band-edge transition was rarely compared quantitatively to the corresponding bulk semiconductor. This is partly due to dielectric screening of the electromagnetic field by QDs, which obscures the underlying optical transition rate, and partly to different quantification of band-edge absorption by an absorption coefficient for bulk semiconductors and an oscillator strength or integrated absorption coefficient for QDs, see Supporting Information S1. To minimize the impact of dielectric screening, we analyzed the absolute absorptance of a series of QD superlattices built from PbSe or CdSe QDs.[15−17] Such samples combine a 0D confinement with a 2D geometry,[18] which makes that only minor corrections are needed for the screening of the electromagnetic field (see also Figure 1). More precisely, we calculated for the different QD samples the local field factor F, which is the ratio between the external and the local electric field using atomistic dielectric modeling (see Supporting Information S8) and found that $|F|^2$ ranges between 0.4 and 0.8. Hence, in terms of dielectric screening, such superlattices indeed form a bridge to quantum wells (Figure 1c), which do not screen the electric field ($|F|^2 = 1$) for perpendicular incidence and exhibit an absorptance $m\pi\alpha$ per allowed transition.

Figure 2a,b presents two monolayer superlattices of epitaxially connected PbSe QDs, one with a square and the other with a silicene-type honeycomb geometry. The high-angle annular dark-field scanning transmission electron microscopy (HAADF-STEM) images of the lattices (in lower right insets) show the atomic connection of QDs via their [100] facets. The electron diffraction patterns (upper right

https://doi.org/10.1021/acs.nanolett.1c02682
Nano Lett. 2021, 21, 9426−9432

insets) reveal that the structures have a high degree of crystallinity, as observed by the occurrence of four and six sharp spots in electron diffraction patterns recorded on a selected area (see Supporting Information S3) for the honeycomb and square superlattices, respectively. The width of the electron diffraction patterns reflects a slight disorder in the alignment of the QDs, as discussed elsewhere.[19] The absorptance spectra of both superlattices are presented in Figure 2c,d. These spectra were measured by placing the samples under a small angle inside the integrating sphere of a UV/vis/NIR spectrometer (see Supporting Information S3.1 for more details). The absorptance spectra shown here are representative for a series of measurements recorded independently by different research groups, see Supporting Information S3. The results are summarized in Table 1. The first absorption feature at ~0.7 eV is indicative of the bandgap transition. As an aside, we remark that two monolayer superlattices stacked on top of each other show an absorptance increased by a factor 2. The right axis of Figure 2c,d present the absorptance corrected for the photonic effects, where the screening of the electromagnetic field is accounted for by the factor $|F|^2$, and reflectance by the factor $4n_m^2/(n_s + n_m)^2$. The maximum absorptances reaches about 3.8 and 4.5% for, respectively, square and honeycomb superlattices. Thus, this is close to two times the absorptance quantum $\pi\alpha$, which is in agreement with the steps calculated for a PbSe quantum well. The absorptance spectra for CdSe honeycomb and square superlattices are presented in Supporting Information S3. In those cases, a first absorptance peak occurs at 2.0 eV, typical for superlattices consisting of CdSe QDs.[16] The absorptance lies between $\pi\alpha$ and $2\pi\alpha$; we expect $m = 1$ for the fundamental absorption in CdSe. It is remarkable that, despite their very different bandgap, degree of quantum confinement, and electronic structure, the absorptance of PbSe and CdSe superlattices at the band-edge transition is very well quantified by $\pi\alpha$.

Table 1. Overview of the Experimental Parameters

configuration	compound	$\mathcal{A}_{exp}$ (%)	$\mathcal{A}_{corr}$ (%)	$\lvert F\rvert^2$	surrounding
honeycomb superlattice	PbSe	1.1	4.5	0.36	$4/(1.44 + 1)^2$
square superlattice	PbSe	1.5	3.8	0.59	$4/(1.44 + 1)^2$
quantum well	PbSe		4.6[a]	1	
honeycomb superlattice	CdSe	1.7	3.4	0.66	$4/(1.46 + 1)^2$
square superlattice	CdSe	1.4	3.2	0.75	$4/(1.46 + 1)^2$

[a]Calculated with tight-binding approach.

HEURISTIC MODEL FOR THE ABSORPTANCE IN A 2D, 0D, AND 3D SEMICONDUCTOR

Above, we showed that the reported absorptance of semiconductor quantum wells, increasing with $m\pi\alpha$ per allowed optical transition, is corroborated by atomistic tight-binding theory. The absorptance quantum also rules the band-edge absorptance of a monolayer of QDs present in a superlattice. We now present a heuristic model that shows that the absorptance quantum per exciton volume is a ruler that unifies the experimental results obtained for 0D quantum dots, 2D quantum wells, and even 3D bulk semiconductors.

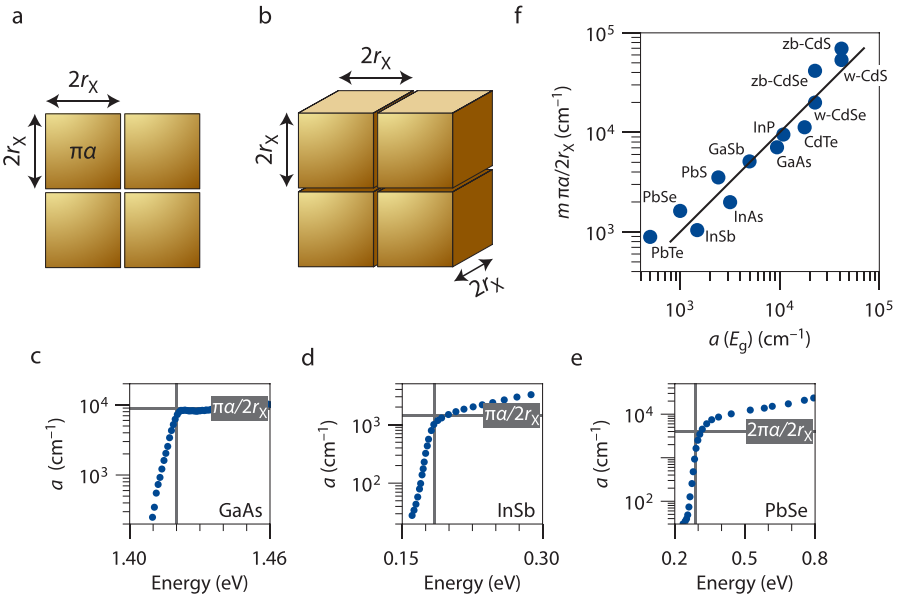

Figure 3. Schematic representation of the heuristic model, and its evaluation for bulk semiconductors. (a) The band edge light absorptance of a quantum well, equal to $m\pi\alpha$ per allowed transition, can be interpreted by dividing the quantum well in square regions with area approximately $4r_X^2$ having an absorptance $m\pi\alpha$ across the exciton binding energy range E_X, see text and eqs 1−3. (b) Extension of this proven concept in the case of bulk semiconductors; this would mean that cubes with edge equal to $2r_X$ have each an absorptance equal to $m\pi\alpha$ per allowed transition, see text and eq 4. (c−e) Experimental check of the above concept by presenting the experimental absorption coefficient spectra for the bulk semiconductors GaAs,[20] InSb,[21] and PbSe,[22] respectively; the vertical gray line shows the bandgap taken from ref 23, the horizontal line shows the value of $m\pi\alpha/2r_X$ with r_X being the bulk exciton Bohr radius taken from ref 23. (f) Experimental check of the concept for a large variety of semiconductors, by plotting $m\pi\alpha/2r_X$ versus the absorption coefficient $a(E_g)$ at the band edge. The black line shows $a(E_g) = m\pi\alpha/2r_X$ with m equal to 1 except for the IV−VI semiconductors for which it is 2.

https://doi.org/10.1021/acs.nanolett.1c02682
Nano Lett. 2021, 21, 9426−9432

We start with the effective mass two-band model for 2D quantum wells,[12] see Supporting Information S1. We consider light absorption from free carrier states $|\nu\rangle$ of the highest valence sub-band induced by the vertical confinement to free carrier states $|c\rangle$ of the lowest conduction sub-band. Excitation involves a monochromatic beam with energy density I, linearly polarized, and normal incidence on the 2D semiconductor, and couples states resonant with the photon energy ($\hbar\omega = E_c - E_v = E_{cv}$). The absorptance is the ratio of the energy absorbed by optical transitions in the semiconductor versus the incident energy, and can be written as

$$\mathcal{A}(\hbar\omega) = \frac{E_{cv}W(\hbar\omega)}{I} = (\pi\alpha)4\pi E_{cv}|\langle c|x|\nu\rangle|^2\rho_{2D}(\hbar\omega) = \sigma_i\rho_{2D}(\hbar\omega) \tag{1}$$

In eq 1, $W(\hbar\omega)$ is the transition rate between the states $|\nu\rangle$ and $|c\rangle$, $\rho_{2D}(\hbar\omega)$ is the joint density of states of optical transitions, and σ_i is the integrated absorption cross section of a single transition (see Supporting Information S1). Within $k\cdot p$ theory, the dipole matrix element $|\langle c|x|\nu\rangle|^2$ is given by $\hbar^2/4\mu E_{cv}$, while ρ_{2D} amounts to $\mu/\pi\hbar^2$ with μ being the reduced effective mass of an electron−hole pair. Substitution of these elements in eq 1 results in the absorptance being equal to $\pi\alpha$ within a single quantum-well sub-band, in agreement with the experimental steps observed for InAs quantum wells.

The density of states $\rho_{2D}(\hbar\omega)$ measures a number of states per unit area and per unit of energy. Interestingly, one can rewrite $\rho_{2D}(\hbar\omega)$ using the Bohr radius r_X, in fact $\sqrt{2}r_X$, as a unit of length and the exciton binding energy E_X as a unit of energy

$$\rho_{2D}(\hbar\omega) = \frac{\mu}{\pi\hbar^2} = \frac{1}{2\pi r_X^2 E_X} \tag{2}$$

Equation 2 suggests that a given 2D semiconductor attains steps $\pi\alpha$ in the absorptance by having $n = 1/2\pi r_X^2$ absorbing transitions per unit area in an energy range E_X. In this regard, a quantum well can thus be represented by a set of active elements, each measuring $2\pi r_X^2$ in area (edges $\sqrt{2\pi}r_x \approx 2r_x$, that is, the exciton Bohr diameter) and exhibiting an absorptance $\pi\alpha$ (or $2\pi\alpha$) across the energy range E_X, see Figure 3a. While different 2D semiconductors will be represented by squares of different sizes, the interplay between the integrated cross section and the 2D density of states always yields the same absorptance steps $\pi\alpha$ (or $2\pi\alpha$). Hence, $\pi\alpha$ can be used as a ruler to quantify σ_i

$$\sigma_i = \frac{\pi\alpha}{\rho_{2D}(\hbar\omega)} = \pi\alpha\frac{\pi\hbar^2}{\mu} \tag{3}$$

Extending this approach to 3D (bulk) semiconductors, we conjecture that for such materials the bulk Bohr diameter of the electron−hole exciton similarly sets the physical volume contributing to a single optical transition. In the heuristic model, this physical volume can be approximated by a cube with edges equal to the Bohr diameter $2r_X$, see Figure 3b. If correct, the absorption coefficient a, that is, the absorptance per unit length, would be given by

$$a = \frac{\mathcal{A}}{2r_X} = \frac{m\pi\alpha}{2r_X} \tag{4}$$

The above relation can be tested by analyzing experimental absorption coefficient spectra for bulk semiconductors from the literature. In Figure 3c−e, we plot such spectra for GaAs,[20] InSb,[21] and PbSe.[22] Similar plots for other semiconductors are collected in Supporting Information S4, (E_{cv} and r_X are from ref 23). It is clear that the crossing of the gray lines (E_{cv}, $\pi\alpha/2r_X$) indicates a point very close to the saturated absorption coefficient at the band edge. For bulk PbSe, we took the value of $2\pi\alpha$ to account for the degeneracy of the band edges (see above). Furthermore, Figure 3f represents $\pi\alpha/2r_X$ versus the absorption coefficient at the band edge for a large variety of semiconductors with very different bandgaps, effective electron and hole mass, and crystal structures. Very remarkably, for a large variety of direct bulk semiconductors with the absorption coefficient spanning over 2 orders of magnitude, $\pi\alpha/2r_X$ is in a reasonable agreement with the absorption coefficient at the band-edge. A more rigorous theoretical approach is outlined in Supporting Information S5, where we introduce the absorptance quantum according to eq 3 as a ruler to quantify absorption spectra of semiconductors. Interestingly, since the transition matrix element to form exciton states can be written in terms of the matrix element $\langle c|x|\nu\rangle$ to form free electron/hole pair states, this ruler approach can be extended to include electron−hole interaction by the formation of unbound excitons. In that case, we obtain a band-edge absorption coefficient of $(\pi\alpha/2r_X)\gamma^2$ with the correction factor γ^2 close to unity, see Supporting Information S5. Clearly, such excitonic effects can contribute to the deviations of the band-edge absorption coefficient of specific semiconductors from the $m\pi\alpha/2r_X$ reference line that is apparent in Figure 3f, in particular for semiconductors such as CdS with large effective masses and small dielectric constants. Otherwise, deviations could be caused by errors on the experimental data or uncertainties on the Bohr diameter.

Extending this approach to 0D QDs, it appears that the volume of a single optical transition is equivalently set by the QD diameter d in the absence of any photonic effects. A QD (superlattice) monolayer would thus have an absorption coefficient $m\pi\alpha/d$ or an absorptance $m\pi\alpha$ for the band-edge transition; this is a conclusion in line with the experimental results shown in Figure 2c,d. In this case, however, the analysis is more complicated because the band-edge transition is heterogeneously broadened to yield an effective density of states $\rho_2(\hbar\omega)$. Considering a Gaussian broadening and writing the QD surface density as n, $\rho_2(\hbar\omega)$ reads

$$\rho_2(\hbar\omega) = n\frac{1}{\sqrt{2\pi}\eta}e^{-(E-(E_c-E_v))^2/2\eta^2} \approx \frac{1}{d^2}\frac{1}{\sqrt{2\pi}\eta}e^{-(E-(E_c-E_v))^2/2\eta^2} \tag{5}$$

Using again the absorptance quantum as a ruler to quantify the integrated cross section (eq 3), the absorptance of a QD monolayer is then obtained as

$$\mathcal{A} = m\pi\alpha\frac{\pi\hbar^2}{\mu d^2}\frac{1}{\sqrt{2\pi}\eta}e^{-(E-(E_c-E_v))^2/2\eta^2} \approx m\pi\alpha\frac{E_Q}{(2\pi)^{3/2}\eta}e^{-(E-(E_c-E_v))^2/2\eta^2} \tag{6}$$

Here, we have introduced the quantization energy E_Q in a QD according to the effective mass model. Interestingly, eq 6 predicts that the band-edge absorptance will peak at $m\pi\alpha$ when the full-width-at-half-maximum of the exciton line is about one-sixth of the quantization energy; a result that agrees quite well with the experimental data shown in Figure 2c,d, and in fact also for most QD suspensions in which the size dispersion is kept to a minimum. Importantly, a more rigorous approach in which we use the known integrated cross section of the PbSe QDs enables us to predict very precisely the absorptance

https://doi.org/10.1021/acs.nanolett.1c02682
Nano Lett. 2021, 21, 9426−9432

spectrum of the epitaxially connected QD films (see Figure 2c,d and Supporting Information S3). We thus conclude that the band-edge absorptance of 0D QDs will indeed peak at around $m\pi\alpha$ for a heterogeneous line broadening typically found with colloidal QDs.

The above observations have important consequences. While any 2D semiconductor exhibits the same absorptance $\pi\alpha$, the absorption coefficient of 3D semiconductors is inversely proportional to the Bohr diameter of the exciton (see eq 4 and Figure 3f); the bulk exciton volume thus determines the widely varying absorption coefficient observed for bulk semiconductors, being the smallest for semiconductors with bands with low effective hole- and electron mass. The absorptance per crystal unit cell will thus increase the strongest for this type of semiconductors when considering the evolution from the 3D case to the 0D case. In practice, the enhanced absorption coefficient of small effective-mass QDs is often cloaked by pronounced dielectric screening. Incorporation of such QDs in a medium with high dielectric constant can therefore strongly enhance the absorptance of light at the band edge, a highly desirable property for their application as LED phosphor or infrared light absorber. The knowledge that a single QD in an appropriate dielectric medium and a semiconductor quantum well both have an absorptance in the range of $\pi\alpha$ is important for the engineering of luminescent light concentrators and photovoltaic devices. To highlight that even one QD monolayer shows sufficient absorption under normal incidence for optoelectronic applications, we present in Supporting Information S6 an infrared photodetector based on a honeycomb monolayer of PbSe QDs; this system has a sufficiently strong light absorptance and at the same time is conducting enough to act as a sensitive photodetector.

For monolayer transition metal dichalcogenide semiconductors, absorptances considerably above $\pi\alpha$ have been reported.[24] This is due the strongly enhanced exciton binding energy. We remark here that for low-dimensional systems, the exciton-binding energy and thus also the enhancement of the absorptance above $\pi\alpha$, may strongly depend on the dielectric function of the environment.[25,26] In this respect, the absorptance of $\pi\alpha$ can be considered as the single particle basis to estimate the enhancement of light absorption if interactions play a role.

The experimental results and model calculations presented here definitely show that photons resonant with the band-edge transition have a probability close to $\pi\alpha$ to be absorbed for each Bohr exciton diameter path length in a semiconductor, independent of whether the exciton is confined in three dimensions, one dimension, or represents a bulk exciton. The heuristic framework that we present provides a basis to understand this compelling generalization. However, a more comprehensive understanding must exist for the observed generality in the absorption strength per exciton Bohr diameter. Also, the finding that for semimetals, such as graphene,[13] and plasmonic systems,[14] the absorptance is equal to $\pi\alpha$ in a very broad energy region further highlights this point.

■ ASSOCIATED CONTENT

Supporting Information

The Supporting Information is available free of charge at https://pubs.acs.org/doi/10.1021/acs.nanolett.1c02682.

Theoretical framework, tight-binding calculations, experimental methods, absorption coefficient spectra of semiconductors, ruler framework, and photodetector example (PDF)

■ AUTHOR INFORMATION

Corresponding Author

Daniel Vanmaekelbergh − *Debye Institute for Nanomaterials Science, Utrecht University, 3584 CC Utrecht, The Netherlands;* orcid.org/0000-0002-3535-8366; Email: d.vanmaekelbergh@uu.nl

Authors

P. Tim Prins − *Debye Institute for Nanomaterials Science, Utrecht University, 3584 CC Utrecht, The Netherlands;* orcid.org/0000-0002-8258-0074

Maryam Alimoradi Jazi − *Debye Institute for Nanomaterials Science, Utrecht University, 3584 CC Utrecht, The Netherlands*

Niall A. Killilea − *Institute - Materials for Electronics and Energy Technology, Materials Science Department, Friedrich-Alexander-Universität Erlangen-Nürnberg, Nürnberg 90429, Germany*

Wiel H. Evers − *Optoelectronic Materials Section, Department of Chemical Engineering, Delft University of Technology, 2629 HZ Delft, The Netherlands*

Pieter Geiregat − *Physics and Chemistry of Nanostructures, Department of Chemistry, Ghent University, B-9000 Ghent, Belgium;* orcid.org/0000-0001-7217-8738

Wolfgang Heiss − *Institute - Materials for Electronics and Energy Technology, Materials Science Department, Friedrich-Alexander-Universität Erlangen-Nürnberg, Nürnberg 90429, Germany;* orcid.org/0000-0003-0430-9550

Arjan J. Houtepen − *Optoelectronic Materials Section, Department of Chemical Engineering, Delft University of Technology, 2629 HZ Delft, The Netherlands;* orcid.org/0000-0001-8328-443X

Christophe Delerue − *University of Lille, CNRS, Centrale Lille, University Polytechnique Hauts-de-France, F-59000 Lille, France;* orcid.org/0000-0002-0427-3001

Zeger Hens − *Physics and Chemistry of Nanostructures, Department of Chemistry, Ghent University, B-9000 Ghent, Belgium;* orcid.org/0000-0002-7041-3375

Complete contact information is available at: https://pubs.acs.org/10.1021/acs.nanolett.1c02682

Author Contributions

[#]P.T.P. and M.A.J. contributed equally to this work.

Author Contributions

P.T.P., M.A.J., A.J.H., and D.V. planned the experiment. P.T.P. and M.A.J. performed the experiments and analyzed the data. M.A.J., N.A.K., and W.H. performed the photoconductivity measurements. W.H.E. and P.G. provided the CdSe samples and measurements. C.D. carried out the atomistic modeling. D.V., Z.H., and C.D. provided the theoretical background for the paper. All authors contributed to the discussions and the manuscript. All authors have given approval to the final version of the manuscript.

Notes

The authors declare no competing financial interest.

https://doi.org/10.1021/acs.nanolett.1c02682
Nano Lett. 2021, 21, 9426−9432

■ ACKNOWLEDGMENTS

D.V. acknowledges support by The Netherlands Organization for Scientific Research (NWO, Grant 14614 "Q-Lumicon") and the European Research Council (ERC Advanced Grant 692691 "First step"). Z.H. acknowledges support by FWO-Vlaanderen (research project 17006602) and Ghent University (BOF-GOA 01G01019). D.V.M, W.H., C.D., and Z.H. acknowledge support from the European Commission via the Marie-Skłodowska Curie action Phonsi (H2020-MSCA-ITN-642656).

■ REFERENCES

(1) Lhuillier, E.; Pedetti, S.; Ithurria, S.; Nadal, B.; Heuclin, H.; Dubertret, B. Two-Dimensional Colloidal Metal Chalcogenides Semiconductors: Synthesis, Spectroscopy, and Applications. *Acc. Chem. Res.* **2015**, *48* (1), 22−30.

(2) Kovalenko, M. V.; Manna, L.; Cabot, A.; Hens, Z.; Talapin, D. V.; Kagan, C. R.; Klimov, V. I.; Rogach, A. L.; Reiss, P.; Milliron, D. J.; Guyot-Sionnnest, P.; Konstantatos, G.; Parak, W. J.; Hyeon, T.; Korgel, B. A.; Murray, C. B.; Heiss, W. Prospects of Nanoscience with Nanocrystals. *ACS Nano* **2015**, *9* (2), 1012−1057.

(3) Coropceanu, I.; Bawendi, M. G. Core/Shell Quantum Dot Based Luminescent Solar Concentrators with Reduced Reabsorption and Enhanced Efficiency. *Nano Lett.* **2014**, *14* (7), 4097−4101.

(4) Lim, J.; Park, Y.-S.; Klimov, V. I. Optical Gain in Colloidal Quantum Dots Achieved with Direct-Current Electrical Pumping. *Nat. Mater.* **2018**, *17* (1), 42−49.

(5) Yang, Z.; Pelton, M.; Fedin, I.; Talapin, D. V.; Waks, E. A Room Temperature Continuous-Wave Nanolaser Using Colloidal Quantum Wells. *Nat. Commun.* **2017**, *8* (1), 143.

(6) Keuleyan, S.; Lhuillier, E.; Brajuskovic, V.; Guyot-Sionnest, P. Mid-Infrared HgTe Colloidal Quantum Dot Photodetectors. *Nat. Photonics* **2011**, *5* (8), 489−493.

(7) Whitham, K.; Yang, J.; Savitzky, B. H.; Kourkoutis, L. F.; Wise, F.; Hanrath, T. Charge Transport and Localization in Atomically Coherent Quantum Dot Solids. *Nat. Mater.* **2016**, *15* (5), 557−563.

(8) Rodina, A. V.; Efros, A. L. Effect of Dielectric Confinement on Optical Properties of Colloidal Nanostructures. *J. Exp. Theor. Phys.* **2016**, *122* (3), 554−566.

(9) Geiregat, P.; Justo, Y.; Abe, S.; Flamee, S.; Hens, Z. Giant and Broad-Band Absorption Enhancement in Colloidal Quantum Dot Monolayers through Dipolar Coupling. *ACS Nano* **2013**, *7* (2), 987−993.

(10) Hens, Z.; Moreels, I. Light Absorption by Colloidal Semiconductor Quantum Dots. *J. Mater. Chem.* **2012**, *22* (21), 10406.

(11) Szkopek, T. The Fine Structure Constant Determines Spontaneous Emission Rates from Semiconductors. *Appl. Phys. Lett.* **2011**, *98* (21), 211117.

(12) Fang, H.; Bechtel, H. A.; Plis, E.; Martin, M. C.; Krishna, S.; Yablonovitch, E.; Javey, A. Quantum of Optical Absorption in Two-Dimensional Semiconductors. *Proc. Natl. Acad. Sci. U. S. A.* **2013**, *110* (29), 11688−11691.

(13) Nair, R. R.; Blake, P.; Grigorenko, A. N.; Novoselov, K. S.; Booth, T. J.; Stauber, T.; Peres, N. M. R.; Geim, A. K. Fine Structure Constant Defines Visual Transparency of Graphene. *Science* **2008**, *320* (5881), 1308−1308.

(14) Kravets, V. G.; Schedin, F.; Grigorenko, A. N. Fine Structure Constant and Quantized Optical Transparency of Plasmonic Nanoarrays. *Nat. Commun.* **2012**, *3* (1), 640.

(15) Evers, W. H.; Goris, B.; Bals, S.; Casavola, M.; de Graaf, J.; van Roij, R.; Dijkstra, M.; Vanmaekelbergh, D. Low-Dimensional Semiconductor Superlattices Formed by Geometric Control over Nanocrystal Attachment. *Nano Lett.* **2013**, *13* (6), 2317−2323.

(16) Boneschanscher, M. P.; Evers, W. H.; Geuchies, J. J.; Altantzis, T.; Goris, B.; Rabouw, F. T.; van Rossum, S. a. P.; van der Zant, H. S. J.; Siebbeles, L. D. a.; Van Tendeloo, G.; Swart, I.; Hilhorst, J.; Petukhov, A. V.; Bals, S.; Vanmaekelbergh, D. Long-Range Orientation and Atomic Attachment of Nanocrystals in 2D Honeycomb Superlattices. *Science* **2014**, *344* (6190), 1377−1380.

(17) Sandeep, C. S. S.; Azpiroz, J. M.; Evers, W. H.; Boehme, S. C.; Moreels, I.; Kinge, S.; Siebbeles, L. D. A.; Infante, I.; Houtepen, A. J. Epitaxially Connected PbSe Quantum-Dot Films: Controlled Neck Formation and Optoelectronic Properties. *ACS Nano* **2014**, *8* (11), 11499−11511.

(18) Walravens, W.; Solano, E.; Geenen, F.; Dendooven, J.; Gorobtsov, O.; Tadjine, A.; Mahmoud, N.; Ding, P. P.; Ruff, J. P. C.; Singer, A.; Roelkens, G.; Delerue, C.; Detavernier, C.; Hens, Z. Setting Carriers Free: Healing Faulty Interfaces Promotes Delocalization and Transport in Nanocrystal Solids. *ACS Nano* **2019**, *13* (11), 12774−12786.

(19) Peters, J. L.; Altantzis, T.; Lobato, I.; Jazi, M. A.; van Overbeek, C.; Bals, S.; Vanmaekelbergh, D.; Sinai, S. B. Mono- and Multilayer Silicene-Type Honeycomb Lattices by Oriented Attachment of PbSe Nanocrystals: Synthesis, Structural Characterization, and Analysis of the Disorder. *Chem. Mater.* **2018**, *30* (14), 4831−4837.

(20) Dell, J. M.; Joyce, M. J.; Usher, B. F.; Yoffe, G. W.; Kemeny, P. C. Unusually Strong Excitonic Absorption in Molecular-Beam-Epitaxy-Grown, Chemically Lifted GaAs Thin Films. *Phys. Rev. B: Condens. Matter Mater. Phys.* **1990**, *42* (15), 9496−9500.

(21) Moss, T. S.; Smith, S. D.; Hawkins, T. D. F. Absorption and Dispersion of Indium Antimonide. *Proc. Phys. Soc., London, Sect. B* **1957**, *70* (8), 776−784.

(22) Scanlon, W. W. Recent Advances in the Optical and Electronic Properties of PbS, PbSe, PbTe and Their Alloys. *J. Phys. Chem. Solids* **1959**, *8* (C), 423−428.

(23) Madelung, O. *Semiconductors: Data Handbook*; Springer Berlin Heidelberg: Berlin, Heidelberg, 2004.

(24) Mak, K. F.; Lee, C.; Hone, J.; Shan, J.; Heinz, T. F. Atomically Thin MoS2: A New Direct-Gap Semiconductor. *Phys. Rev. Lett.* **2010**, *105* (13), 136805.

(25) Chernikov, A.; Berkelbach, T. C.; Hill, H. M.; Rigosi, A.; Li, Y.; Aslan, O. B.; Reichman, D. R.; Hybertsen, M. S.; Heinz, T. F. Exciton Binding Energy and Nonhydrogenic Rydberg Series in Monolayer WS2. *Phys. Rev. Lett.* **2014**, *113* (7), 076802.

(26) Li, Y.; Chernikov, A.; Zhang, X.; Rigosi, A.; Hill, H. M.; van der Zande, A. M.; Chenet, D. A.; Shih, E.-M.; Hone, J.; Heinz, T. F. Measurement of the Optical Dielectric Function of Monolayer Transition-Metal Dichalcogenides: MoS2, MoSe2, WS2, WSe2. *Phys. Rev. B: Condens. Matter Mater. Phys.* **2014**, *90* (20), 205422.

https://doi.org/10.1021/acs.nanolett.1c02682
Nano Lett. 2021, 21, 9426−9432